# A proof of concept simulator including dynamic interactions in dense suburban railway context

Mehdi Baali*[1], Rémi Coulaud[2], and Christine Buisson[3]

[1]Research engineer, SNCF, France
[2]Head of Datalab' Mass Transit, SNCF Voyageurs, France
[3]Senior researcher, LICIT-ECO7, Université Gustave Eiffel & ENTPE, France

## Short summary

Dense suburban railway systems are subject to various types of hazards whose effects on supply and demand interact at short time scales: dynamic interactions. The combination of hazards and dynamic interactions may lead delays to propagate and worsen, which significantly deteriorates the system's performance. As such, it is crucial to simulate these effects to design robust schedules. However, existing simulators for dense suburban railway systems do not fully include demand-to-supply and supply-to-demand dynamic interactions. In this paper, a proof of concept simulator is presented to show the importance of considering demand-to-supply and supply-to-demand dynamic interactions. Compared to a benchmark simulator that neglects these dynamic interactions, on the presented case study, our simulator is able to highlight additional phenomena resulting from demand-to-supply and supply-to-demand dynamic interactions. In practice, the implementation of all dynamic interactions in a ready-to-use simulator will significantly improve future scheduling. This work is a first step toward this goal in which a proof of concept is provided.
**Keywords**: Demand, Disruption, Public Transport, Railway, Simulation, Supply

## 1 Introduction

Urban sprawl in big cities has challenged existing transport modes for commuting between the suburbs and the city center. People need high-performance public transport systems to travel large distances twice a day. Metros, generally underground, are often confined to the city center and nearby suburbs. Differing from metros, suburban trains are often used to connect more distant suburbs to the city center. However, these transport systems also need to be robust. A robust system is a system that has the ability to maintain or recover, by itself, a decent performance after a small hazard (Goverde & Hansen, 2013; Jensen, 2015; Lusby et al., 2018). The robustness of a transport system is generally assessed using simulators considering the specificities of the underlying transport mode.
Suburban trains and metros are close transport systems: both depend on railways, and both have high capacities. However, they differ in four main points (that may not be true for all networks, as the separation between train and metro is rather fluid).

1. Train infrastructure is generally shared between many train lines and can also be shared between several train types. Metro lines circulate in segregated infrastructures.

2. Train lines may be composed of several branches. Services may also vary: omnibus services (serving all stations), semi-direct services (serving some stations but not all), and direct services (serving only the termini). Metro lines have a restricted number of branches and services, usually only one.

3. Train operations are generally schedule-based, which means that a train is not allowed to depart from a station before its scheduled departure time. Metro operations are headway-based, which means that metros leave the origin terminus with a fixed headway and run without schedules.

4. Trains are often run with a lower frequency than metros, and with higher differences in services during peak periods and off-peak periods.

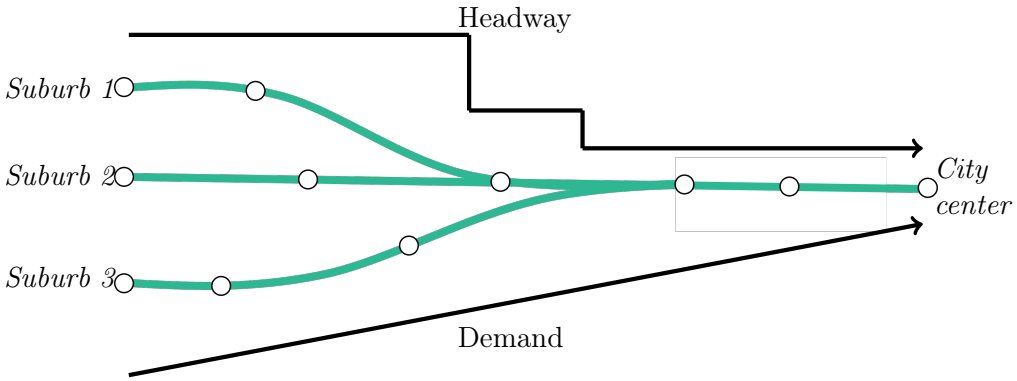



Figure 1: Archetype of a dense suburban train line with a terminus in the city center. Headway decreases while approaching the city center due to the merging of the branches. Demand increases while approaching the city center due to an increasing urban density.

Dense suburban railway systems have similarities to the metros (Altazin, 2018). Their infrastructure is open to other trains, but in nominal situations, they are essentially dedicated to a single train line. The train line is generally made up of several branches that run between a single city center and several parts of the suburbs. The demand at the branches is generally lower, so the frequency is less, and this justifies the operation to be schedule-based to minimize the waiting time spent by passengers for a given train. The demand in the central section is generally higher due to higher urban densities. At the same time, trains from the different branches merge, resulting in higher frequencies, frequencies generally as high as that of a metro. Figure 1 shows an archetype of a dense suburban train line.

In such a line, fluctuations related to operations (running times or dwell times) (Yuan et al., 2010; Buchmüller et al., 2008) or passenger demand (Pan et al., 2017) are numerous and dynamically interact between them. This leads delays to appear more frequently and to propagate more easily compared to other types of train systems.

Interactions between supply and demand appear at short-term scale (dynamic interactions): for example, between one vehicle and the vehicle directly after, between one station and the next station, or between one vehicle and its demand. Dynamic interactions are of four types:

- Supply-to-supply dynamic interactions, related to signaling (Zieger et al., 2018; Huang et al., 2024);
- Demand-to-demand dynamic interactions, related to boarding failure (Leurent et al., 2014; Hänseler et al., 2020; Cornet, 2020) ;
- Demand-to-supply dynamic interactions, related to dwell time delays that may appear when the alighting and boarding volumes are too large (Cornet et al., 2019; Palmqvist et al., 2020; Coulaud et al., 2023; Baali, Buisson, et al., 2025);
- Supply-to-demand dynamic interactions, related to passenger arrival behaviors that can be split into headway-based passengers (who arrive uniformly at the station, knowing a train will arrive shortly) and schedule-based passengers (aiming for a train scheduled at a specific time) (Baali et al., 2026).

These dynamic interactions (illustrated in Figure 2) have been extensively studied in the literature. However, understanding them is not sufficient to solve operational performance and robustness issues. They need to be addressed through simulation tools. Existing simulators are limited to other transport modes, such as buses or metros (Toledo et al., 2010; Fonzone et al., 2015; Srikukenthiran & Shalaby, 2017; D'Acierno et al., 2017), or do not consider all dynamic interactions (Landex & Nielsen, 2006; Cornet, 2020; Othman et al., 2023). To our knowledge, no simulator for dense suburban train systems that integrates all dynamic interactions exists so far.

Therefore, the goal of this work is to provide a proof of concept simulator for dense suburban trains. The proof of concept will help highlight several phenomena related to supply-to-demand and demand-to-supply dynamic interactions that cannot be spotted without considering them.

The paper is structured as follows. First, a simulator integrating all dynamic interactions is presented along with a benchmark simulator. Then, a comparison is provided between both simulator results for a case study in Paris. This paper ends with a conclusion.

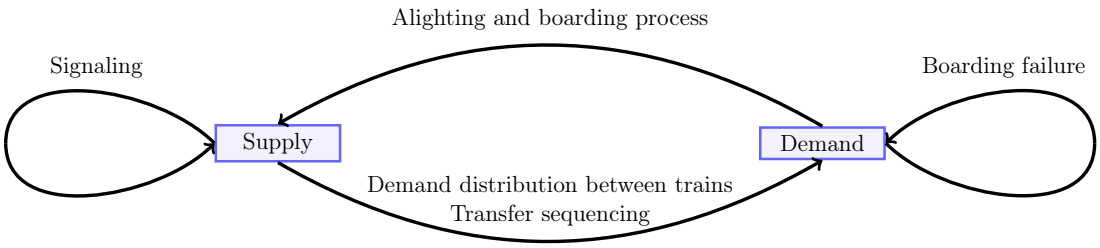



Figure 2: Scheme of the dynamic interactions between supply and demand in the case of Mass Transit train systems. Some interactions are not specific to Mass Transit train systems.

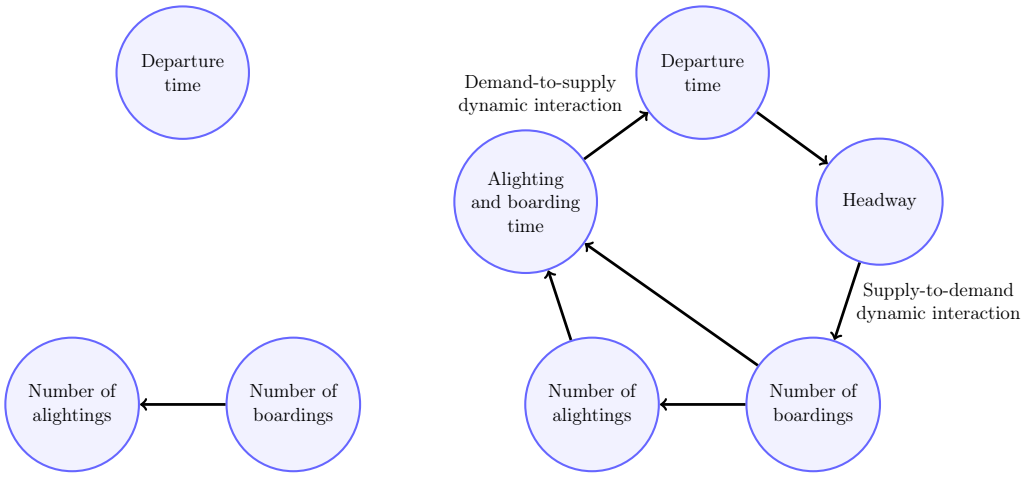



Figure 3: Framework of the benchmark simulator (left) and our simulator (right) and dependencies between the variables. The dependencies lead to cyclic equations.

## 2 Methodology

In the literature, railway simulator commonly do not consider all dynamic interactions. Supply-to-supply dynamic interactions are integrated but demand and supply are considered separately. A simplified version of such a simulator will serve as a benchmark in this work (Figure 3 right). By contrast, we present a simplified simulator considering all the dynamic interactions (Figure 3 right). This simplified simulator is only a proof-of-concept The comparison between both simulators will serve to demonstrate the ability of our simulator to simulate phenomena that typically result from supply-to-demand and demand-to-supply dynamic interactions.

***A simplified benchmark simulator***

To illustrate the relevance of considering dynamic interactions in the simulator, we implement a simulator that only considers supply-to-supply dynamic interactions, similarly to most existing railway simulators.

**Number of alightings** First, the number of alightings $A$ from each train $k$ at each station $s$, is obtained from passengers who have previously boarded $B$ using an origin-destination matrix $m^{OD}$. The origin-destination matrix is assumed to be deterministic and independent of the date $d$. The perimeter will focus only on the morning peak hours, and then the matrix is assumed to be independent of the time of day. The matrix depends on the train index $k$, but only via the service. If a station is skipped by train index $k$, no one will alight there. All trains running the same service are assumed to have the same origin-destination matrix.

$$\tilde{A}_{k,s,d} = \sum_{s'<s} m^{OD}_{s',s,k} \tilde{B}_{k,s',d}. \tag{1}$$

**Number of boardings** The number of boardings is proportional to the total number of entries $E_{s,d}$. This number of entries is distributed between the different trains with a rate $\beta_k$ which only depends on the train index.

$$\tilde{B}_{k,s,d} = \beta_k E_{s,d}. \tag{2}$$

**Departure time** The observed departure time only depends on the scheduled departure time, the train ahead (supply-to-supply dynamic interaction), and some constant potential margin consumption in case of delay. This latter term is independent of alighting and boarding volumes, meaning that no demand-to-supply dynamic interaction is considered contrary to our simulator.

$$\tilde{t}^{obs}_{k,s,d} = \max\left(t^{sch}_{k,s}, \tilde{t}^{obs}_{k-1,s,d} + h^{min}, \tilde{t}^{obs}_{k,s-1,d} + (t^{sch}_{k,s} - t^{sch}_{k,s-1}) - M\right). \tag{3}$$

***A simplified simulator with dynamic interactions***

To demonstrate the importance of the dynamic interactions, we built a simplified simulator considering all dynamic interactions to be compared with the benchmark simulator.

**Number of alightings** The number of alightings is computed similarly to what is done with the benchmark simulator.

$$A_{k,s,d} = \sum_{s'<s} m^{OD}_{s',s,k} B_{k,s',d} \tag{4}$$

**Number of boardings** The number of boardings $B$ is computed in two steps. In a first step, the boarding demand $B^O_{k,s,d}$ (number of passengers who want to board train $k$ at station $s$ on date $d$) is obtained using the behavior-based model from Baali et al. (2026) which accounts for supply-to-demand dynamic interactions. In this model, the boarding demand is split into schedule-based (SB) passengers and headway-based (HB) passengers. Schedule-based passengers aim for a specific train and arrive close to the scheduled departure time. Headway-based passengers arrive uniformly at the station within the headway, knowing that the frequency is high enough to avoid waiting too long. Headway-based passengers generate an additional boarding demand when the headway increases, which is why this distinction is crucial. Similarly to what is done for the benchmark simulator, the boarding demand ($B^O_{k,s,d}$) is assumed to be linear with the total number of entries $E_{s,d}$ in the station, allowing for variations in demand from one date to another. $q^{SB}_{k,s}$ represents the rate of schedule-based passengers, and $q^{HB}_{k,s}$ the rate of headway-based passengers.

$$B^O_{k,s,d} = \left(q^{SB}_{k,s} + q^{HB}_{k,s} h^{obs}_{k,s,d}\right) E_{s,d} \tag{5}$$

In a second step, to get the effective number of boardings ($B_{k,s,d}$) from the boarding demand ($B^O_{k,s,d}$), one has to consider the number of boarding failures. Boarding failures ($\Delta B_{k,s,d}$) correspond to passengers who cannot board the train $k$ for which they arrived, because the load ($L_{k,s,d}$) of the train cannot exceed the train passengers capacity ($C$). This illustrates demand-to-demand dynamic interactions.

$$B_{k,s,d} = \min\left(B^O_{k,s,d} + \Delta B_{k-1,s,d}, C - L_{k,s,d} - A_{k,s,d}\right) \tag{6}$$

$$\Delta B_{k,s,d} = L_{k,s,d} + A_{k,s,d} + B^O_{k,s,d} + \Delta B_{k-1,s,d} - C \tag{7}$$

Notice that, in the case study, the train capacity (2,592 P) is high enough (compared to the boarding demands) to completely prevent boarding failures from appearing.

**Headway** $h^{obs}_{k,s,d}$ is the observed headway, i.e., the difference between the observed departure time $t^{obs}_{k,s,d}$ of the train and the observed departure time of the previous train.

$$h^{obs}_{k,s,d} = t^{obs}_{k,s,d} - t^{obs}_{k-1,s,d}. \tag{8}$$

| Quantity | Name | Type | Unit | Value |
|---|---|---|---|---|
| $A$ | Number of alightings | Variable | [P] | |
| $B$ | Number of boardings | Variable | [P] | |
| $h$ | Headway between two trains | Variable | [s] | |
| $t^{obs}$ | Observed departure time | Variable | [s] | |
| $ABT$ | Alighting and boarding time | Variable | [s] | |
| $B^O$ | Boarding demand | Variable | [P] | |
| $\Delta B$ | Number of boarding failures | Variable | [P] | |
| $L$ | Train load | Variable | [P] | |
| $m^{OD}$ | Origin-destination matrix | Parameter | Without unit | Context dependent |
| $q^{SB}$ | Schedule-based passenger rate | Parameter | Without unit | Context dependent |
| $q^{HB}$ | Headway-based passenger rate | Parameter | $[\mathrm{s}^{-1}]$ | Context dependent |
| $C$ | Train passengers capacity | Parameter | [P] | 2,592P |
| $h^{min}$ | Minimal headway (due to signaling) | Parameter | [s] | 120s |
| $TT$ | Technical time | Parameter | [s] | 7.5s |
| $\zeta$ | Critical door ratio | Parameter | | 0.15 |
| $\psi$ | Flow size | Parameter | $[\mathrm{P}\cdot\mathrm{s}^{-1}]$ | $4.9\mathrm{P}\cdot\mathrm{s}^{-1}$ |
| $\gamma$ | Density calibration parameter | Parameter | $[\mathrm{P}^{-\frac{1}{2}}]$ | $0.09\mathrm{P}^{-\frac{1}{2}}$ |
| $M$ | Constant margin (benchmark) | Parameter | [s] | 8s |
| $t^{sch}$ | Schedule departure time | Parameter | [s] | Context dependent |
| $E$ | Total number of entry | Parameter | [P] | Context dependent |
| $RT$ | Running time | Parameter | [s] | Context dependent |

Table 1: Quantities considered in the simulation.

**Departure time** The observed departure time $t^{obs}_{k,s,d}$ is determined by three constraints: either the train has to wait for its scheduled departure time $t^{sch}_{k,s,d}$ before leaving (nominal situation), or it has to wait until the previous train is far enough according to a minimal headway $h^{min}$ due to signaling (which is a simplified modeling of supply-to-supply dynamic interactions), or it is limited by the observed running time $RT^{obs}$ and the observed alighting and boarding time $ABT^{obs}$ (plus a constant technical time corresponding to the time for opening/closing the doors and dispatching).

$$t^{obs}_{k,s,d} = \max\left(t^{sch}_{k,s}, t^{obs}_{k-1,s,d} + h^{min}, t^{obs}_{k,s-1,d} + RT_{k,s,d} + ABT_{k,s,d} + TT\right) \tag{9}$$

**Alighting and boarding time** Finally, the alighting and boarding time $ABT$, is assumed to only depend on the number of alightings $A_{k,s,d,j}$ and the number of boardings $B_{k,s,d,j}$ at the critical door (door $j$ where the number of alightings and boardings is maximal). This corresponds to demand-to-supply dynamic interactions. The ratio between the total number of movements at the critical door and over the entire train ($\zeta_s = \frac{\max(A_{k,s,d,j}+B_{k,s,d,j})}{A_{k,s,d}+B_{k,s,d}}$) is assumed to be constant for each station and each train. From there, the alighting and boarding time is computed using the deterministic model of Baali, Buisson, et al. (2025) and the method of Baali, Kuipers, et al. (2025).

$$ABT_{k,s,d} = \frac{1}{0.8}\int_0^{0.8\zeta_s(A_{k,s,d}+B_{k,s,d})} \frac{1}{\psi\left(1-\exp(-\gamma\sqrt{\zeta_s(A_{k,s,d}+B_{k,s,d})-N})\right)\left(\exp(-\gamma\sqrt{\zeta_s(A_{k,s,d}+B_{k,s,d})-N})\right)} dN. \tag{10}$$

Notice that there exist dependencies due to other lines or branches. Trains from other lines or branches may hinder trains from the studied line due to signaling (supply-to-supply dynamic interactions), but we will neglect them in this work.

The above-presented equations are cyclic because they depend on each other. As a reminder, Figure 3 illustrates the dependencies between the variables. To solve this, the computation for any ($k$, $s$, $d$) is done twice iteratively. First, the demand-to-supply dynamic interaction is neglected (the alighting and boarding time is assumed to be zero). Then, the observed departure time, headway, and number of boardings are computed from there. Based on the computed number of boardings, the observed departure time is computed again with the demand-to-supply dynamic interaction (influence of the alighting and boarding time). Finally, all quantities are computed again based on this updated value of the observed departure time.

Among all above-presented quantities: $m^{OD}$, $q^{SB}$, $q^{HB}$, $C$, $h^{min}$, $TT$, $t^{sch}$, $E$, and $RT$ are constant parameters. The other quantities are variables determined by the equations (see Table 1 for a summary of the notations).

| Scenario | Description |
|---|---|
| 10-year | The demand has homogeneously increased by 9% per year |
| 10-year_small_disruption | 10-year scenario and a 3-minute delay appears before train 4 arrives at *Meudon* |
| 10-year_exceptional_demand | 10-year scenario with an additional 1.5-time homogeneous increase in demand |

Table 2: Scenarios studied with deterministic analyses.

The parameters of both simulators are fixed at the same value (see Table 1). The comparison between these two simulators will highlight how supply-to-demand and demand-to-supply dynamic interactions impact operations at the stop level.

## 3 Results and discussion

### *Case study*

The case study presented in this work takes place on a Paris suburban train line (*line N*). The case study consists of studying the effect of the arrival of *Metro 15* (part of the *Grand Paris Express*) at *Clamart* on the operation of *line N* (part of the existing suburban railway network) around *Clamart*. More specifically, we focus on *Clamart*, *Meudon* (one station before), and *Vanves-Malakoff* (one station ahead).
The case study focuses on the direction toward Paris between 7:15 am and 8 am.
The case study is 10 years from now (when *Metro 15* will be fully open). The simulated transport plan is close to the 2025 transport plan, with one omnibus service (service that stops at all stations) every 15 minutes and one semi-direct service (service that does not stop at all stations) every 15 minutes. Contrary to the 2025 transport plan, all services stop at *Clamart*.
The number of entries in the stations studied is computed based on realistic current orders of magnitude with an increase of +9% every year (+9% was the increase between 2022 and 2023), and +9% every year at *Clamart*. Notice that this increase is plausible but probably overestimated, as it is based on a value from the post-COVID recovery period.
Similarly, the origin-destination matrix is inspired by the current one with an arbitrary increase of *Clamart* as a destination.
Finally, based on the data analysis made by Ingvardson et al. (2018) (in Denmark) and Baali et al. (2026) (in the Paris region), a headway-based proportion of 40% is chosen for *Meudon* and *Vanves-Malakoff*, and 60% for *Clamart*.

### *Studied scenarios*

Three scenarios are discussed. In addition to this increase in demand assumed for a 10 years ahead horizon, we will test the effect of a small disruption (+3 minutes in running time for train 3 at *Meudon*), and the effect of an exceptional demand (a 1.5-time homogeneous increase in demand throughout the studied line). The scenarios are summarized in Table 2. For each scenario, we compare the simulated response of the train system with our simulator and with the benchmark in space-time diagrams.

### *Simulation results*

Figure 4 shows the space-time diagram for simulated trains with both simulators for the 10-year scenario. With the resulting increase in demand, the benchmark simulator pretends that no delay occurs. In contrast, our simulator shows small delays from *Clamart* and downstream on all omnibus trains. Some delays also appear on semi-direct trains, but their magnitude is much lower. This is due to the headway before omnibus trains, which is higher and induces a significant number of headway-based passengers to board the train. These significant numbers of headway-based boardings increase the dwell time and cause dwell time delays.
Figure 5 shows the space-time diagram for simulated trains with both simulators for the 10-year_small_disruption scenario. The benchmark simulator shows that the delay propagates down-

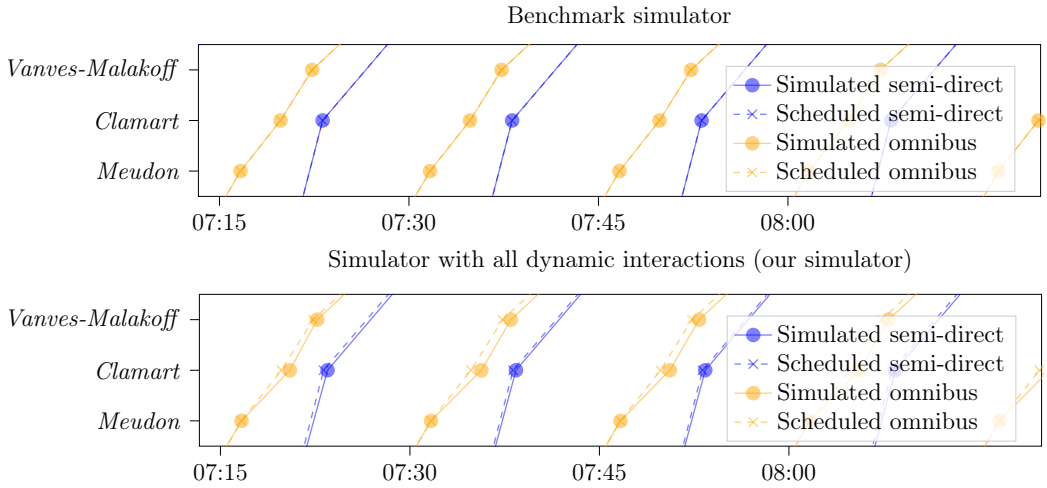



Figure 4: Space-time diagram for simulated trains with the benchmark simulator (top) and our simulator (bottom) for the 10-year scenario. Small dwell time delays appear on omnibus trains at *Clamart* with our simulator. The benchmark simulator does not reproduce the dwell time delays due to the increase in demand.

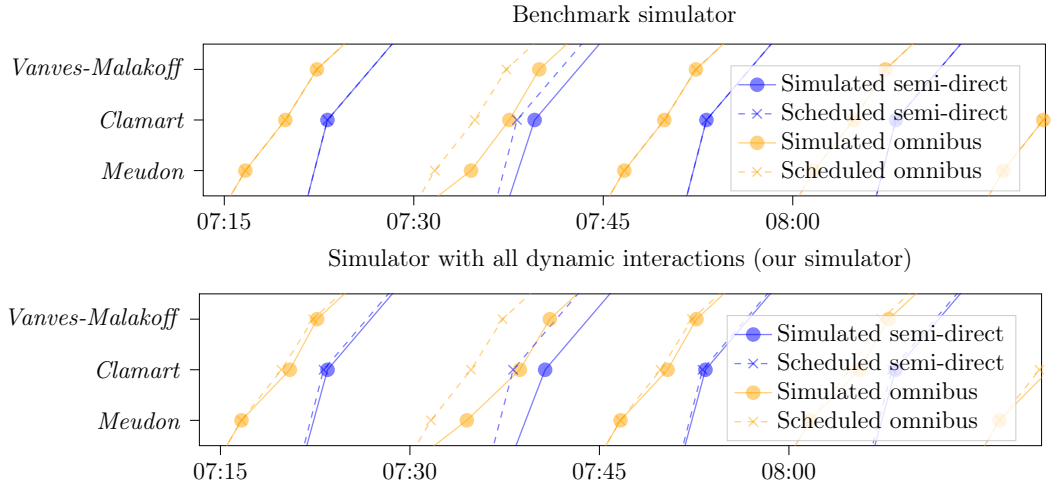



Figure 5: Space-time diagram for simulated trains with the benchmark simulator (top) and our simulator (bottom) for the 10-year_small_disruption scenario. The impact of the disruption is worse with our simulator, for the impacted train and the following semi-direct train. The following omnibus train suffers less delay than in the case without disruption (see Figure 4).

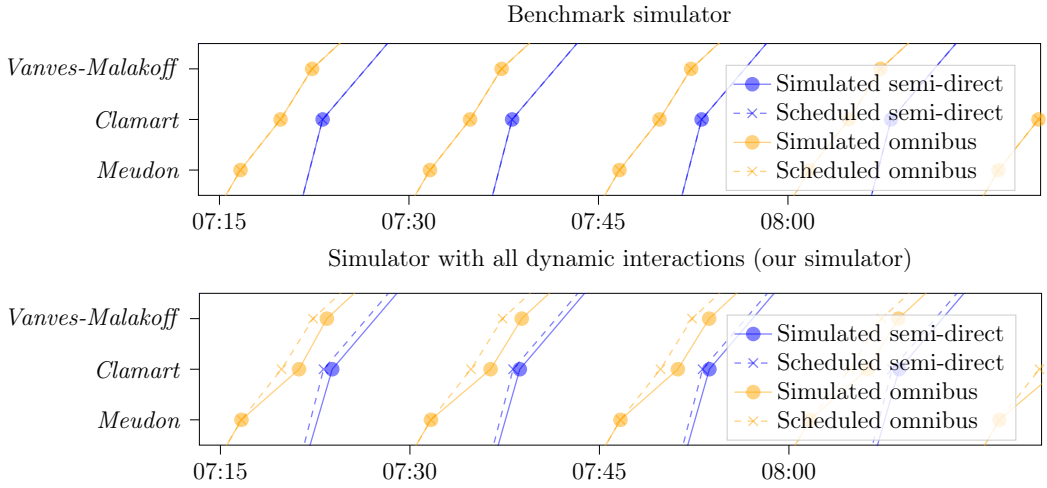



Figure 6: Space-time diagram for simulated trains with the benchmark simulator (top) and our simulator (bottom) for the year_exceptional_demand scenario. The benchmark simulator does not reproduce the large dwell time delays due to the increase in demand.

stream in the train, but slowly decreases using margins that are assumed to be consumed to catch up. The delay is high enough to also propagate to the next train due to supply-to-supply dynamic interactions. The delay propagation stops after the next train because there is enough space between the train slots. Considering all dynamic interactions in our simulator, the resulting delay is of higher magnitude and worsens downstream due to the increase in headway (leading to more boarding passengers and then dwell time delays). The following semi-direct train is also delayed due to the supply-to-supply dynamic interactions, but the following omnibus train suffers less delay than in the 10-year scenario (Figure 4) due to a reduced headway.
Figure 6 shows the space-time diagram for simulated trains with both simulators for the 10-year_exceptional_demand scenario. Similar to the 10-year scenario, the benchmark simulator shows no delay occurring, while large delays are observed considering all dynamic interactions in our simulator. These delays are, moreover, significantly higher than in the 10-year scenario.

## 4 Conclusions

In this work, we proposed a proof of concept of a simulator that considers all dynamic interactions in dense suburban train contexts. This simulator was compared to a benchmark that ignored demand-to-supply and supply-to-demand dynamic interactions. The comparison was performed via a case study on *line N* in the context of the arrival of *Metro 15* at *Clamart*.
Among the highlighted phenomena typically related to demand-to-supply and supply-to-demand dynamic interactions, we showed a significant propensity for dwell time delays and overcrowding when demand increases at a station with many headway-based passengers and substantial variation in headways. We also showed that a disruption right before this type of station leads to an increase in demand, also resulting in dwell time delays and overcrowding.
Although, the presented simulator is only a simplified one, this preliminary work indicates that developing a comprehensive simulator is promising. Such a simulator would satisfy the need for more reliable estimations of the effect of dynamic interactions between supply and demand on operational performance and robustness.

## References

Altazin, E. (2018). *Stabilité et replanification d'un système ferroviaire dense* (Doctoral Dissertation). Université de Lyon.

Baali, M., Buisson, C., Coulaud, R., & Daamen, W. (2025). Modeling the alighting and boarding process through train doors using a markov process with flow-dependent transition

probabilities. *Physica A: Statistical Mechanics and its Applications*, 130942. doi: 10.1016/j.physa.2025.130942

Baali, M., Coulaud, R., & Buisson, C. (2026). *Estimation of the impact of short train delays on the demand distribution between trains, based on passenger arrival behaviors.* (Under review)

Baali, M., Kuipers, R., Coulaud, R., Buisson, C., & Palmqvist, C.-W. (2025). Long enough but not too long: a posteriori determination of the dwell time margins from high-resolution passenger flow data. *Data Science for Transportation*, *7*(2), 7. doi: 10.1007/s42421-025-00121-9

Buchmüller, S., Weidmann, U., & Nash, A. (2008). Development of a dwell time calculation model for timetable planning. *WIT Transactions on The Built Environment*, *103*, 525–534.

Cornet, S. (2020). *Formalisation et résolution du problème de construction de grilles horaires robustes pour les réseaux ferrés denses* (Doctoral Dissertation). Université de Lille.

Cornet, S., Buisson, C., Ramond, F., Bouvarel, P., & Rodriguez, J. (2019). Methods for quantitative assessment of passenger flow influence on train dwell time in dense traffic areas. *Transportation Research Part C: Emerging Technologies*, *106*, 345–359. doi: 10.1016/j.trc.2019.05.008

Coulaud, R., Keribin, C., & Stoltz, G. (2023). Modeling dwell time in a data-rich railway environment: with operations and passenger flows data. *Transportation Research Part C: Emerging Technologies*, *146*, 103980. doi: 10.1016/j.trc.2022.103980

D'Acierno, L., Botte, M., Placido, A., Caropreso, C., & Montella, B. (2017). Methodology for determining dwell times consistent with passenger flows in the case of metro services. *Urban Rail Transit*, *3*, 73–89. doi: 10.1007/s40864-017-0062-4

Fonzone, A., Schmöcker, J.-D., & Liu, R. (2015). A model of bus bunching under reliability-based passenger arrival patterns. *Transportation Research Procedia*, *7*, 276–299. doi: 10.1016/j.trpro.2015.06.015

Goverde, R. M., & Hansen, I. A. (2013). Performance indicators for railway timetables. In *2013 ieee international conference on intelligent rail transportation proceedings* (pp. 301–306). doi: 10.1109/ICIRT.2013.6696312

Hänseler, F. S., van den Heuvel, J. P., Cats, O., Daamen, W., & Hoogendoorn, S. P. (2020). A passenger-pedestrian model to assess platform and train usage from automated data. *Transportation Research Part A: Policy and Practice*, *132*, 948–968. doi: 10.1016/j.tra.2019.12.032

Huang, P., Guo, J., Liu, S., & Corman, c., Fran. (2024). Explainable train delay propagation: A graph attention network approach. *Transportation Research Part E: Logistics and Transportation Review*, *184*, 103457. doi: 10.1016/j.tre.2024.103457

Ingvardson, J. B., Nielsen, O. A., Raveau, S., & Nielsen, B. F. (2018). Passenger arrival and waiting time distributions dependent on train service frequency and station characteristics: A smart card data analysis. *Transportation Research Part C: Emerging Technologies*, *90*, 292–306. doi: 10.1016/j.trc.2018.03.006

Jensen, L. W. (2015). *Robustness indicators and capacity models for railway networks* (Unpublished doctoral dissertation). DTU Management.

Landex, A., & Nielsen, O. A. (2006). Modelling expected train passenger delays on large scale railway networks. In *7 th world congress on railway research.*

Leurent, F., Chandakas, E., & Poulhès, A. (2014). A traffic assignment model for passenger transit on a capacitated network: Bi-layer framework, line sub-models and large-scale application. *Transportation Research Part C: Emerging Technologies*, *47*, 3–27. doi: 10.1016/j.trc.2014.07.004

Lusby, R. M., Larsen, J., & Bull, S. (2018). A survey on robustness in railway planning. *European Journal of Operational Research*, *266*(1), 1–15. doi: 10.1016/j.ejor.2017.07.044

Othman, N. B., Jayaraman, V., Chan, W., Loh, Z. X. K., Rajendram, R., Mepparambath, R. M., ... Qin, Z. (2023). Summit: A multi-modal agent-based co-simulation of urban public transport with applications in contingency planning. *Simulation Modelling Practice and Theory*, *126*, 102760. doi: 10.1016/j.simpat.2023.102760

Palmqvist, C.-W., Tomii, N., & Ochiai, Y. (2020). Explaining dwell time delays with passenger counts for some commuter trains in stockholm and tokyo. *Journal of Rail Transport Planning & Management*, *14*, 100189. doi: 10.1016/j.jrtpm.2020.100189

Pan, H., Li, J., Shen, Q., & Shi, C. (2017). What determines rail transit passenger volume? implications for transit oriented development planning. *Transportation Research Part D: Transport and Environment*, *57*, 52–63. doi: 10.1016/j.trd.2017.09.016

Srikukenthiran, S., & Shalaby, A. (2017). Enabling large-scale transit microsimulation for disruption response support using the nexus platform: proof-of-concept case study of the greater toronto area transit network. *Public Transport*, *9*(1), 411–435. doi: 10.1007/s12469-017-0158-y

Toledo, T., Cats, O., Burghout, W., & Koutsopoulos, H. N. (2010). Mesoscopic simulation for transit operations. *Transportation Research Part C: Emerging Technologies*, *18*(6), 896–908. doi: 10.1016/j.trc.2010.02.008

Yuan, J., Goverde, R., & Hansen, I. (2010). Evaluating stochastic train process time distribution models on the basis of empirical detection data. *WIT Transactions on State of the Art in Science and Engineering*, *40*, 95–104.

Zieger, S., Weik, N., & Nießen, N. (2018). The influence of buffer time distributions in delay propagation modelling of railway networks. *Journal of Rail Transport Planning & Management*, *8*(3-4), 220–232. doi: 10.1016/j.jrtpm.2018.09.001